

## 4.2. FORECASTING THE SPECTRAL AMPLITUDES OF STRONG EARTHQUAKE GROUND MOTION

M.D. Trifunac<sup>I</sup>

### SYNOPSIS

A new method for the empirical scaling of spectral amplitudes of recorded strong earthquake ground motion is proposed. The advantages of the proposed approach are that (1) the spectra can be estimated directly in terms of the parameters which are routinely available to earthquake engineering, seismological and geological communities all over the world and (2) the uncertainties associated with scaling of spectral amplitudes in terms of peak acceleration are completely eliminated.

### INTRODUCTION

Characterization of strong shaking at a point involves detailed description of time dependent amplitude and frequency content. For engineering applications this description can be reduced to a characterization in terms of response spectra and the frequency dependent duration of shaking. The analysis of duration or the equivalent number of stress reversals of known amplitudes becomes essential for the design of non-linear yielding systems and should be considered in every non-linear analysis. This topic has been discussed in a separate paper<sup>1</sup> and will not be repeated here. In this paper we will examine only the amplitude characterization of strong shaking as portrayed by response spectra.

There are essentially two ways in which strong shaking is currently described in engineering applications. The first one involves earthquake magnitude,  $M$ , distance between the source and the station,  $R$ , and in some cases certain geometric characteristics of the fault (e.g., length, width, depth). This approach seems to be preferred where some even limited statistical information is available on earthquake occurrence (e.g. Western United States and Japan). The second method is or can be related to an estimate of the Modified Mercalli Intensity (M.M.I. or its equivalent) at the site and is typically utilized in those areas of the world where little or no data is available on earthquake magnitudes. By using some empirical relationship between the epicentral intensity and earthquake magnitude this approach is often transformed to a format which resembles the first method. This inevitably involves some judgment or reliance on poorly defined empirical correlations between magnitude and intensity and thus increases the uncertainties in the final results.

All these empirical relationships, developed for engineering applications, are based on data gathered by accurate strong-motion recorders. Such instruments are now capable of recording in the frequency range from 0.05 cps to about 50 cps and may reach the dynamic range of up to about 60 db. Over 1500 records of this type have, so far, been gathered all over the world and are representative of strong shaking caused by earthquakes in the magnitude range from between about  $M=3$  and  $M=7.5$ , for the epicentral distances from about 10 km to some 300 km and for the M.M.I. range between about III and IX. Time and amplitude characteristics of these records depend on the source mechanism, on the propagation path, on the geology surrounding the station and on the local characteristics of the recording station. When an adequate number of simultaneous records is available it is possible to study some details of the source characteristics<sup>2,3,4,5</sup> of the transmission path<sup>6</sup> and of the effects of local geologic conditions<sup>7</sup>. Such studies have revealed a high degree of

---

<sup>I</sup> Associate Professor, Civil Engineering, University of Southern California, Los Angeles, California 90007

complexity and a considerable range of possible values for many parameters that govern the properties of the source mechanism and the wave propagation path. It has been learned<sup>8</sup> that one of the simple and physically sound ways of describing the source mechanism might be in terms of the seismic moment  $M_0 = \mu A_0 \bar{u}$  (where  $\mu$  represents rigidity of the material surrounding the fault,  $A_0$  is the fault area and  $\bar{u}$  is the dislocation amplitude averaged over the fault surface) and the stress drop,  $\sigma$ . The number of earthquakes that has been studied in some detail<sup>2,3,4,5</sup> however, is still very limited because of the inadequate number of strong-motion records and unless many more instruments are deployed and maintained over the next several decades there is little chance that this situation will be improved. Therefore, even though it seems that it will be possible to develop models for prediction of strong shaking in terms of all the important parameters which describe the earthquake source it may take many years before a sound statistical basis is developed for calibration of these parameters in a given geologic environment and for semi-deterministic prediction of the characteristics of strong shaking. Current research<sup>4,5</sup> has indicated that the deterministic modeling of earthquake sources may already be feasible for long waves (long periods, approximately  $>1$  sec) but much research still remains to be done to understand the intermediate and short period range of strong shaking in real time. It seems appropriate then to explore what can be done now with the available data and simplified characterization of the earthquake source.

#### SPECTRA WITH FIXED SHAPE

Following the introduction of the concept of response spectra into earthquake engineering in 1930's<sup>9,10</sup> this format of describing the amplitudes of strong shaking has gained considerable popularity in engineering applications<sup>11,12</sup>. Beginning in mid 1950's and until early 1970's accelerograph recordings were employed to compute response spectra which then served as a basis for the development of "standard" spectral shapes for use in the design (Fig. 1). These spectra have fixed shape, independent of earthquake magnitude, source to station distance and the recording site conditions. Their amplitudes can represent normalized average spectra<sup>11</sup> or an envelope of spectra of specially selected representative records<sup>12</sup> and are scaled in terms of a single parameter, which could be selected to represent spectral intensity or more often, peak acceleration. It has been recognized that the shape of response spectra depends on earthquake magnitude, the distance of recording station<sup>11</sup> and the geologic and soil characteristics underneath the recording station<sup>13,14</sup>, but until recently the number of uniformly processed strong-motion accelerograms was not adequate to examine even some preliminary empirical models which would reflect all these effects simultaneously.

#### SPECTRA WITH VARIABLE SHAPE

With an increase in the number of recorded strong-motion accelerograms in late 1960's and early 1970's it became possible to carry out preliminary investigations of more detailed spectral characteristics. An example of this<sup>13</sup> is shown in Fig. 2 where the spectral shapes now depend on the type of soil conditions underneath the station and on whether average or average plus one standard deviation of normalized amplitudes are selected for scaling. These spectral shapes, however, still do not depend explicitly on other parameters (e.g. earthquake magnitude and distance) and their overall amplitudes are still determined by the estimates of peak acceleration only. There are well known uncertainties associated with forecasting the expected peak acceleration, peak velocity and peak displacement which result when a complex phenomenon such as strong ground motion is characterized by a single peak or even by a "representative" set of peaks<sup>15,16</sup>.

To avoid these difficulties it is proposed here to address the problem of scaling response spectra directly and in terms of only those parameters which are readily available to engineering, geological and seismological communities all over the world. On the basis of practical considerations it seems worthwhile to divide the input parameters into two groups: (1) Earthquake magnitude,  $M$ , epicentral distance,  $R$ , recording site conditions,  $s$ , component direction,  $v$ , and the desired confidence level  $p$ ; and (2) Modified Mercalli Intensity,  $I_{MM}$ , recording site conditions,  $s$ , component direction,  $v$ , and the confidence level,  $p$ . Here the recording site conditions are grouped roughly into three categories: (1)  $s=0$  for stations recording on alluvium or sedimentary rocks, (2)  $s=2$  for stations on sound basement rocks and (3)  $s=1$  for intermediate sites<sup>17</sup>. Parameter  $v$  is selected to be 0 for horizontal and 1 for vertical motions. The linearized confidence level  $p$  (e.g. 0.90) is utilized to determine what percentage (e.g. 90%) of spectra is expected to lie below the selected empirical spectrum. It should be emphasized that the above two proposed groups of parameters should not be interpreted as representing the final, complete or even the most useful set of scaling factors. Ideally spectral shapes should be forecast in terms of those quantities which have direct relation to the physics of the problem at the earthquake source (for example, moment and stress drop). However, these are not yet computed on a routine basis and their determination requires considerable research effort for each earthquake. On the other hand, the earthquake magnitude (instrumental) and intensity scales (qualitative, descriptive) are used all over the world and are systematically gathered into catalogues and statistical tables on earthquake occurrence. Thus until we reach a stage in our scientific and technological development when there will exist detailed statistical data on more meaningful and accurate parameters for scaling earthquake sources it seems worthwhile to examine the possibility of developing preliminary scaling functions which will predict response spectra directly in terms of the available information (e.g. groups (1) or (2)).

Different types of spectra are used in earthquake engineering: (a) Absolute acceleration spectra, SA, (b) relative velocity spectra, SV, (c) relative displacement spectra, SD and (d) Pseudo velocity spectra, PSV. In strong-motion seismology Fourier spectra, FS, are most frequently employed. For brevity in this presentation we will examine some characteristics of the absolute acceleration spectra, SA, only. Many properties of these spectra are closely related to the characteristics of other spectra not discussed in this paper.

#### Forecasting absolute acceleration spectra in terms of $I_{MM}$ , $s$ , $v$ and $p$

M.M.I. scale and its equivalents represent subjective and qualitative description of the severity of strong earthquake ground motion at a point, a shorthand description of damage, and have no direct physical basis which would allow their representation by numerical scales. Approximate empirical correlations show, however, that if one arbitrarily assigns linearly distributed numerical values from 1 to 12 to the twelve descriptive levels of M.M.I. scale, that certain quantitative characteristics can be assigned to each level. Moreover, it appears that the linearly increasing values from 1 to 12 seem to be adequate for most preliminary correlations.<sup>16</sup> By utilizing an approach which is analogous to the correlation proposed for scaling Fourier Amplitude Spectra<sup>18</sup> one can write

$$\log_{10}[SA(T),p] = a(T)p + b(T)I_{M.M.} + c(T) + d(T)s + e(T)v, \quad (1)$$

where  $SA(T),p$  represents the absolute acceleration spectrum amplitude at the period of the single-degree-of-freedom oscillator,  $T$ , which will exceed 100p percent of all spectra recorded under identical conditions.  $p$  represents the

confidence level and  $I_{M.M.}$  stands for M.M.I. level. Functions  $a(T)$ ,  $b(T)$ , ... and  $e(T)$  can be determined by a method analogous to that developed for Fourier amplitude spectra<sup>18</sup> and for any desired value of  $\zeta$ , representing fraction of critical damping. Figure 3 presents functions  $a(T)$  through  $e(T)$  for five values of  $\zeta = 0.0, 0.02, 0.05, 0.10$  and  $0.20$ . Function  $a(T)$  describes the width of the distribution of the spectral amplitudes at different periods. For the 10% to 90% confidence intervals it shows the spectral amplitudes varying by about one order of magnitude (factors ranging from 5 to about 15). The minimum spread is found for the periods between  $T = 0.3$  sec and  $T = 1$  sec and then increases for periods shorter than  $T = 0.3$  sec and larger than  $T = 1$  sec. Similar correlations but based on earthquake magnitude,  $M$ , and epicentral distance,  $R$ , rather than M.M.I. (observed at the recording station) lead to comparable amplitudes of  $a(T)$  for intermediate and short periods and larger  $a(T)$  for periods larger than about 2 to 3 sec (Fig. 5). This means that the spectral amplitudes can be predicted, by using as simple an empirical model as (1), with comparable or, for some periods, even better confidence than with the model in terms of earthquake magnitude and epicentral distance. Considering the qualitative and descriptive nature of M.M.I. this result is remarkable. Function  $b(T)$  is nearly constant, equal to about 0.3, and decreases toward 0.2 for period longer than 2 to 3 sec. For the interval of intensities where (1) applies, M.M.I. between about IV and VIII, this means that this model suggests an increase of spectral amplitudes for each level of M.M.I. scale equal to about 0.3 on logarithmic scale. Function  $d(T)$  is positive for periods shorter than about 1 sec. This means that the high frequency spectral amplitudes are larger on hard basement rock sites ( $s=2$ ) than on alluvium sites ( $s=0$ ). This trend is consistent with similar analyses dealing with Fourier amplitude spectra<sup>18</sup>. All these correlations show that the largest and the smallest amplitudes of  $d(T)$  differ by as much as 0.3 on logarithmic scale. Several correlations with M.M.I.<sup>16,17</sup> however, have a tendency to yield larger differences between  $s=0$  and  $s=2$  in the high-frequency range than the correlations with magnitude and distance<sup>15,18</sup>. This results in the zero crossing of  $d(T)$  in the period range close to about 1 sec. for correlations with M.M.I. (Fig. 3) and in the period range of 0.2 to 0.3 sec for correlations with magnitude and distance (Fig. 5).

An example of absolute acceleration spectrum computed from (1) for a selected set of scaling parameters and with amplitudes normalized to  $g$  ( $981 \text{ cm/sec}^2$ ) is shown in Fig. 4. Spectral amplitudes for intensity levels assigned to numerical values 4 to 8 and corresponding to M.M.I. levels IV, VI and VIII are shown in heavy lines to indicate the range of amplitudes for which (1) is valid and for which most recordings are now available. Spectral amplitudes for M.M.I. levels equal to X and XII (light lines) have been plotted for illustration purpose only and are outside the range for which model (1) applies. Fig. 4 also shows the average and average plus one standard deviation of acceleration spectra that result from the overall digitization noise in processing strong-motion accelerograms. It is seen that the signal to noise ratio reduces for periods longer than about 2 sec. and for lower levels of shaking.

The functional form of equation (1) has been selected purposely so as not to include the dependence of spectral amplitudes on the epicentral distance. An introduction of maximum (epicentral) intensity or the epicentral distance into (1) would be expected to increase the accuracy of this approach which would then be reflected in some decrease of the amplitudes of  $a(T)$ . On the other hand such refinement would further limit the applicability of (1) to Western United States and to California in particular, because the rate of attenuation of seismic waves is known to depend on the characteristics

of the geologic path traversed by the waves and the attenuation of strong shaking in California is implicitly included in all analyses which are based on the data recorded there. Correlations with M.M.I. at the recording station only should, at least in principle, be more applicable to other seismic regions, provided it is feasible to develop correlations indicating the amount and the type of variation in determining intensity levels in different parts of the country and worldwide.

Forecasting absolute acceleration spectra in terms of M, R, s, v and p

Again extending the work on the scaling of Fourier amplitude spectra<sup>18</sup> to correlations of absolute acceleration spectra, one can write

$$\log_{10} [SA(T), p] = M + \log_{10} A_0(R) - a(T)p - b(T)M - c(T) - d(T)s - e(T)v - f(T)M^2 - g(T)R. \quad (2)$$

It is seen that in this equation M (earthquake magnitude) corresponds to I<sub>M.M.</sub> in (1). Additional terms,  $\log_{10} A_0(R)$  (same as  $\log_{10} A_0(\Delta)$  in reference 20),  $f(T)$  and  $g(T)$ , now model the attenuation with increasing epicentral distance, R, decreasing rate of growth of spectral amplitudes for large M and correction to  $\log_{10} A_0(R)$  that may result from the frequency dependent anelastic attenuation. As in the correlations of Fourier amplitude spectra<sup>18</sup> with M, R, s, v and p, equation (2) is assumed to be valid in the magnitude interval between  $M_{\min}$  and  $M_{\max}$  where  $M_{\min} \equiv -b(T)/2f(T)$  and  $M_{\max} \equiv [1 - b(T)]/2f(T)$ . For  $M > M_{\max}$  the term  $f(T)M^2$  is to be replaced by  $f(T)(M - M_{\max})^2$  and for  $M < M_{\min}$ , M is replaced by  $M_{\min}$  in all terms which appear to the right of  $\log_{10} A_0(R)$  in equation (2). This formulation approximately describes the fact that now appears to be indicated by the strong-motion observations and which is that the near-field spectral amplitudes essentially cease to grow for magnitudes in the range of and greater than 7. Direct correlations with computed acceleration spectra lead to  $a(T)$ ,  $b(T)$ ... and  $g(T)$ , for different values of  $\zeta$ , as shown in Fig. 5. Function  $a(T)$  decreases from about -1.0 for small T to about -1.6 for  $T \approx 10$  sec.  $b(T)$ ,  $c(T)$  and  $f(T)$  describe the parabolic portion of equation (2) between  $M_{\min}$  and  $M_{\max}$ .  $d(T)$  and  $e(T)$  are very similar to their counterparts in Fig. 3.  $g(T)$  is small, about -0.001, so that even for the epicentral distances in excess of 100 km the spectral shape is not changed appreciably.

Figure 6 presents an example of absolute acceleration spectra computed from (2) and for the set of scaling parameters shown in the figure. It shows the diminishing rate of growth of spectral amplitudes with respect to earthquake magnitude. This trend is in good agreement with the analyses of the near-field spectra<sup>8</sup> which show that close to the fault the stress drop and the dislocation amplitude are the principal scaling parameters for spectral amplitudes. The duration of strong shaking, however, is expected to continue to grow with earthquake magnitude<sup>1</sup>.

Equations (1) and (2) can be utilized to study the relationships between selected fixed shape spectra (e.g. Fig. 1) and the variable shape spectra. By normalizing SA(T) in (1) and (2), so that the amplitudes at  $T = 0.04$  sec are equal to one, it is possible to cast the variable shape spectra into a format where spectral amplitudes could be scaled by peak acceleration. An example of this is shown in Fig. 7. The shape of the resulting spectra will, of course, depend on all parameters which enter into equations (1) and (2) but for simplicity in Fig. 7 the changes with respect to M and s only are illustrated. The dependence of spectral shapes on site conditions is as expected from the nature of function  $d(T)$  in Figure 5. The amplitudes and the transition period where spectra for  $s = 2$  intersect spectra for  $s = 0$

are both influenced by the normalization which requires all spectral amplitudes to converge to unity for  $T = 0.04$  sec. The changes in spectral shapes with magnitude are less obvious from the analysis of  $b(T)$ ,  $c(T)$  and  $f(T)$  in Figure 5, and agree with the expectations based on the source mechanism theory<sup>8</sup>, which also leads to higher energy content in the long waves (longer periods  $T$ ) for greater magnitudes. Clearly, in the development of the fixed shape spectra for use in earthquake resistant design, decisions must be made how to average or envelope normalized response spectra and how to scale the overall spectral amplitudes. The use of the fixed shape spectra in design would imply that the effects on spectral shape of other parameters ( $M$ ,  $R$ ,  $s$ ,  $v$  and  $p$  or  $I_{M.M.}$ ,  $s$ ,  $v$  and  $p$ ) scale up linearly with peak acceleration. For consistency with other approximations, before such simplifications are adopted, it seems worthwhile to examine their engineering, economical and safety related consequences.

#### CONCLUSIONS

The new method for scaling absolute acceleration spectra, as presented in this paper, can only be considered as a preliminary test on how response spectra might be scaled and what scaling parameters could be utilized for that purpose. The 186 recorded accelerograms which provide the basis for this work are obviously far from adequate to characterize the complete range of all parameters adopted for this purpose. Nevertheless the work presented here, and other similar correlations now being developed should help in the selection of better empirical models in future work and in the selection of the optimum number and type of scaling parameters.

The shortcomings associated with the use of simple correlations (1) and (2) are many, have been discussed in part elsewhere<sup>1,8</sup> and need not be repeated here. It seems clear however, that a methodology for the estimation of the spectral amplitudes directly in terms of the routinely available information is possible. This approach does not only avoid the difficulties which are associated with the selection of the peak acceleration but also eliminates the necessary averaging over other parameters which is implied by other methods which use fixed<sup>11,12</sup> or variable<sup>13</sup> shape spectra. Two unexpected results of this analysis are: (1) that the spectral shapes do not seem to change considerably with distance from the source (i.e.  $g(T)$  is small) and (2) that the scaling of spectral amplitudes in terms of M.M.I. does not lead to greater scatter of estimates (as measured by  $a(T)$ ) than the scaling in terms of earthquake magnitude and source to station distance. This second conclusion is certainly influenced by the selection of the approximate empirical models (1) and (2) but it seems unlikely that it will change much when other better models become available.

#### REFERENCES

1. Westermo, B. and M.D. Trifunac (1977). Recent Developments in the Analysis of the Duration of Strong Earthquake Ground Motion, Sixth World Conf. Earthquake Eng., New Delhi, India.
2. Trifunac, M.D. (1972). Stress Estimates for San Fernando, California Earthquake of February 9, 1971: Main event and thirteen aftershocks, Bull. Seism. Soc. Am. 62, 721-750.
3. Trifunac, M.D. (1972). Tectonics Stress and Source Mechanism of the Imperial Valley, California, earthquake of 1940, Bull. Seism. Soc. Am. 62, 1283-1302.

4. Trifunac, M.D. (1974). A Three-dimensional Dislocation Model for the San Fernando, California, earthquake of February 9, 1971, *Bull. Seism. Soc. Am.* 64, 149-172.
5. Trifunac, M.D. and F. E. Udvardia (1974). Parkfield, California, earthquake of June 27, 1966: a three-dimensional moving dislocation, *Bull. Seism. Soc. Am.* 64, 511-533.
6. Udvardia F. E. and M.D. Trifunac (1974). Variations of Strong Earthquake Ground Shaking in the Los Angeles area, *Bull. Seism. Soc. Am.* 64, 1429-1454.
7. Wong H.L. and M.D. Trifunac (1977). A Note on the Effects of Recording Site Conditions on Amplitudes of Strong Earthquake Ground Motion, Sixth World Conf. Earthquake Eng., New Delhi, India.
8. Trifunac, M.D. (1973). Analysis of Strong Earthquake Ground Motion for Prediction of Response Spectra, *Int. Journ. of Earthquake Eng. and Struct. Dyn.* 2, 59-69.
9. Benioff, H. (1934). The Physical Evaluation of Seismic Destructiveness, *Bull. Seism. Soc. Am.* 24, 398-403.
10. Biot, M.A. (1941). A Mechanical Analyzer for the Prediction of Earthquake Stresses, *Bull. Seism. Soc. Amer.* 31, 151-171.
11. Housner, G. W. (1970). Design Spectrum, Chapter 5 in *Earthquake Engineering*, edited by R. L. Wiegell, Prentice-Hall.
12. U.S. Nuclear Regulatory Commission (1973). Design Response Spectra for Seismic Design of Nuclear Power Plants, Regulatory Guide 1.60, Washington, D.C. : Directorate of Regulatory Standards.
13. Seed, H.B., C. Ugas and J. Lysmer (1976). Site-dependent Spectra for Earthquake-resistant design, Earthquake Engineering Res. Center, EERC 74-12, U.C. Berkeley.
14. Gutenberg, B. (1957). Effects of Ground on Earthquake Motion, *Bull. Seism. Soc. Amer.* 47, 221-250.
15. Trifunac, M.D. (1975). Preliminary Analysis of the Peaks of Strong Earthquake Ground Motion - dependence of Peaks on Earthquake Magnitude, Epicentral Distance and the Recording Site Conditions, *Bull. Seism. Soc. Amer.* 66, 189-219.
16. Trifunac, M.D. (1976). A Note on the Range of Peak Amplitudes of Recorded Accelerations, Velocities and Displacements with Respect to the Modified Mercalli Intensity, *Earthquake Notes*, Vol. 46, No.2.
17. Trifunac, M.D. and A. G. Brady (1975). On the Correlation of Seismic Intensity Scales with the Peaks of Recorded Strong Ground Motion, *Bull. Seism. Soc. Am.* 65, 139-162.
18. Trifunac, M.D. (1976). Preliminary Empirical Model for Scaling Fourier Amplitude Spectra of Strong Ground Acceleration in terms of Earthquake Magnitude Source to Station Distance and Recording Site Conditions, *Bull. Seism. Soc. Amer.* 66, 1343-1373.
19. Trifunac, M.D., F. E. Udvardia and A.G. Brady (1973). Analysis of Errors in Digitized Strong Motion Accelerograms, *Bull. Seism. Soc. Amer.* 63, 157-187.
20. Trifunac, M.D. (1977). An Instrumental Comparison of the Modified Mercalli (M.M.I.) and Medvedev-Karnik-Sponheuer (M.K.S.) Intensity Scales, Sixth World Conf. Earthquake Eng., New Delhi, India.

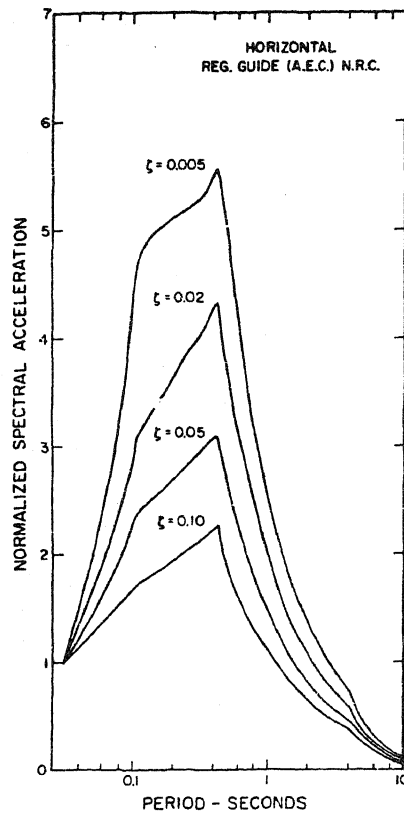


FIGURE 1

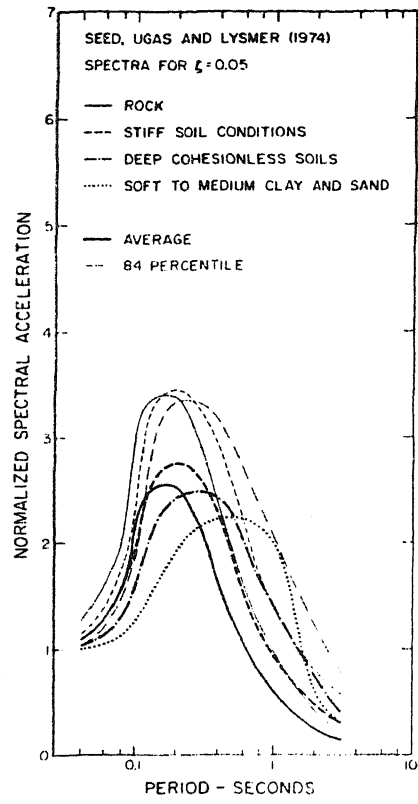


FIGURE 2

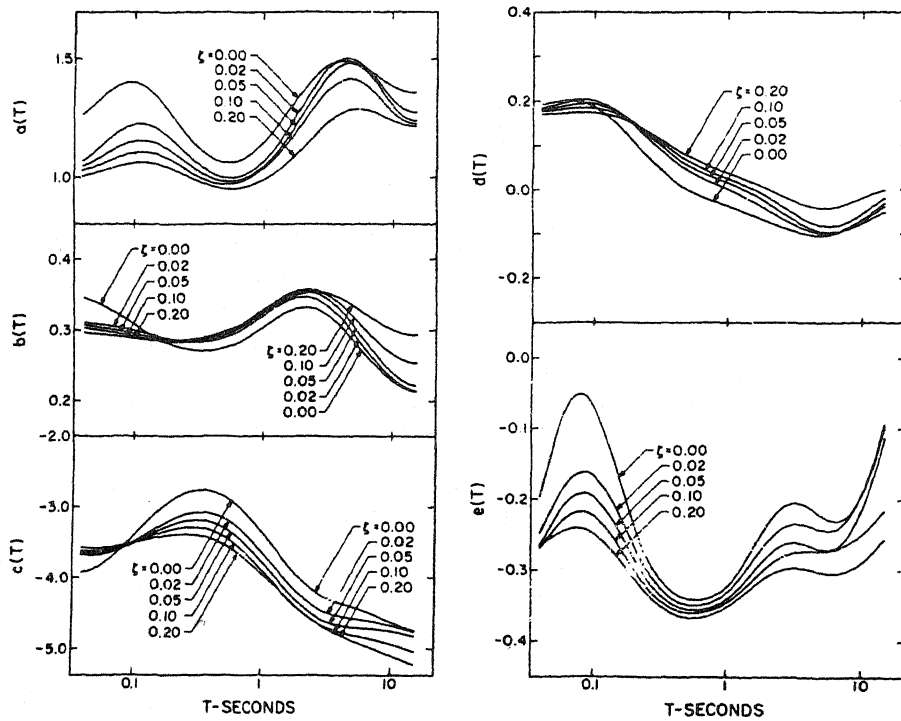


FIGURE 3



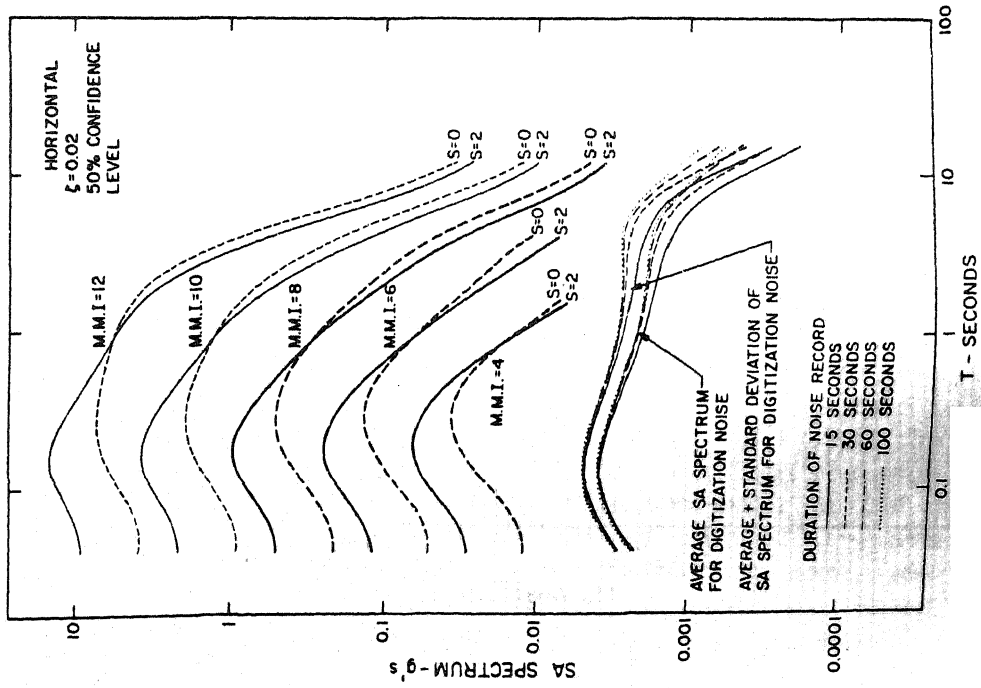


FIGURE 4

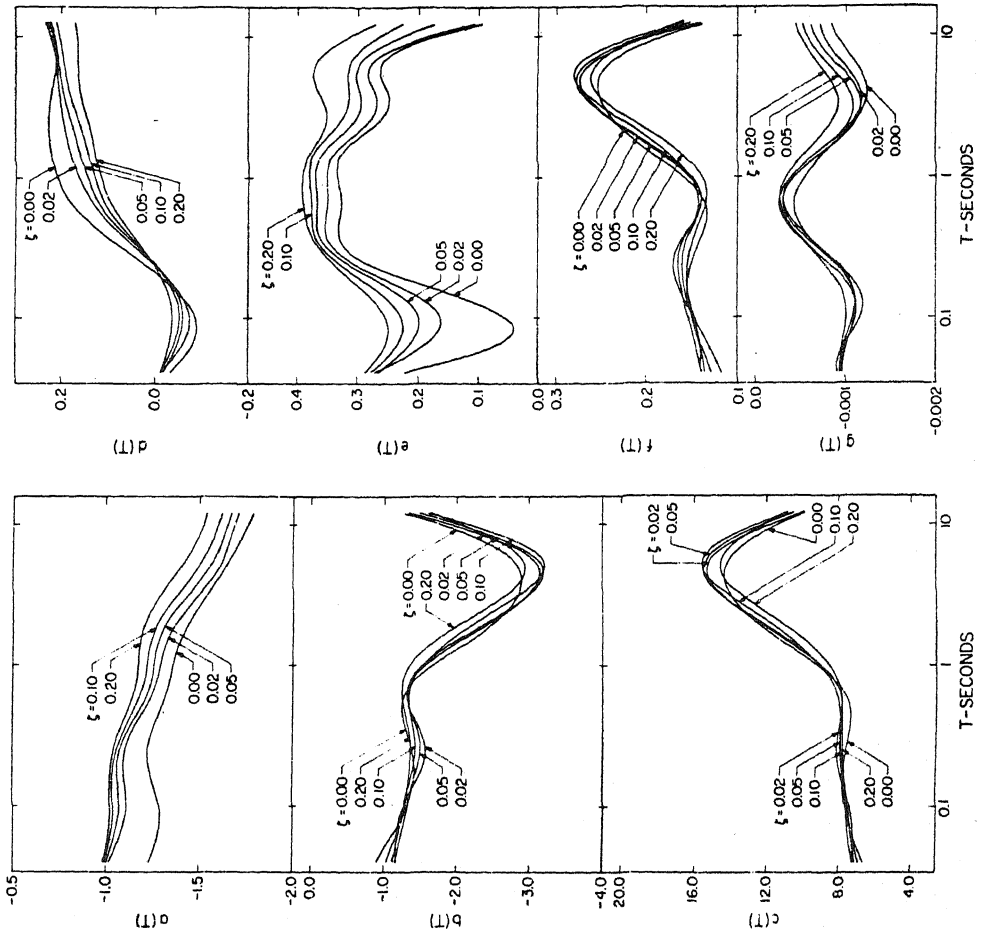


FIGURE 5

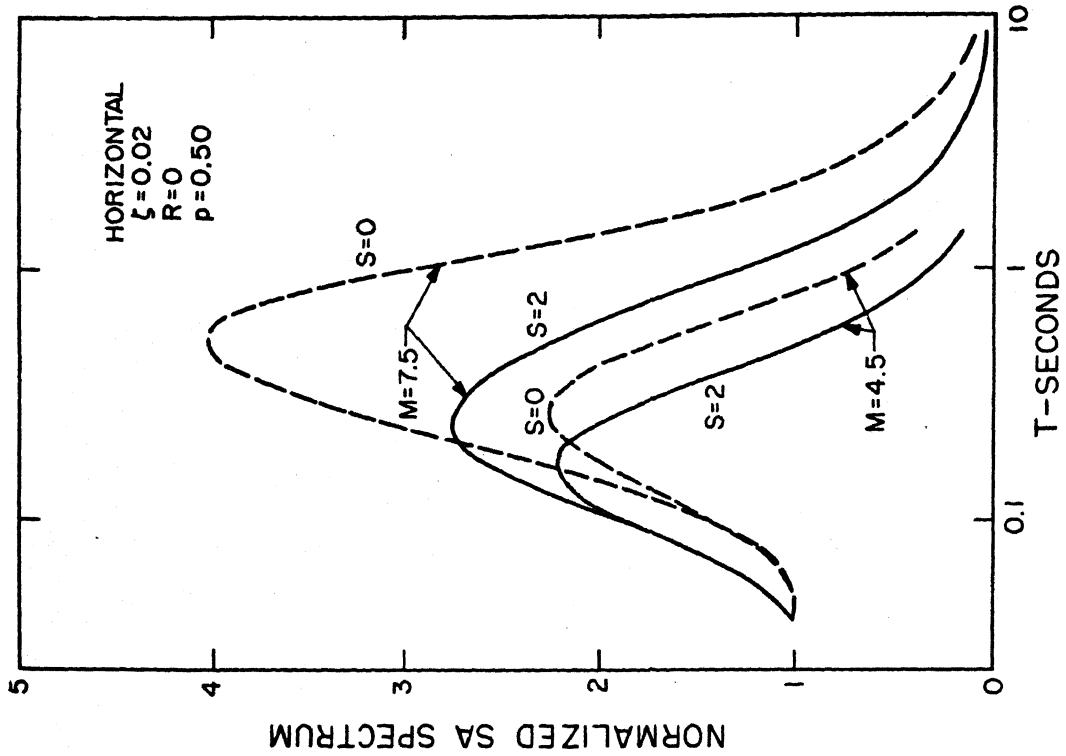


FIGURE 7

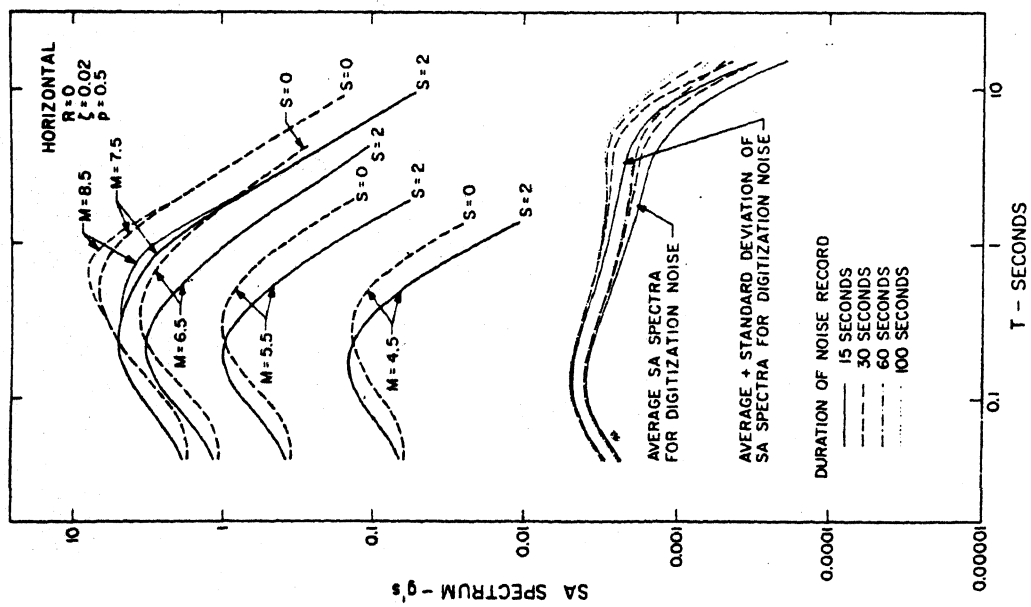


FIGURE 6